AFCRL-72-0256

RIES 71-32

RELAXATION PROCESSES IN EXPANDING FLOWS OF COMBUSTION PRODUCTS

by

Frederick P. Boynton

and

Edward R. Fisher

Research Institute for Engineering Sciences
Wayne State University
Detroit, Michigan 48202

Contract No. F19628-72-C-0007
Project No. 8692

SPECIAL REPORT

July 1971

Contract Monitor: Alva T. Stair,Jr.
Optical Physics Laboratory

Approved for public release; distribution unlimited.

Sponsored by
Advanced Research Projects Agency
ARPA Order No. 1856
Monitored by
AIR FORCE CAMBRIDGE RESEARCH LABORATORIES
AIR FORCE SYSTEMS COMMAND
UNITED STATES AIR FORCE
BEDFORD, MASSACHUSETTS 01730

Program code no.....2E50

Effective date of contract.....12 July 1971

Contract expiration date.....16 October 1972

Principal investigator and phone no.....Dr. Adolf R. Hochstim/313 577-3867

Project scientist and phone no.....Dr. Alva T. Stair, Jr./617 861-4911

UNCLASSIFIED
Security Classification

DOCUMENT CONTROL DATA - R & D
(Security classification of title, body of abstract and indexing annotation must be entered when the overall report is classified)

1. ORIGINATING ACTIVITY (Corporate author)
WAYNE STATE UNIVERSITY
RESEARCH INSTITUTE FOR ENGINEERING SCIENCES
DETROIT, MICHIGAN 48202

2a. REPORT SECURITY CLASSIFICATION
UNCLASSIFIED

2b. GROUP

3. REPORT TITLE
RELAXATION PROCESSES IN EXPANDING FLOWS OF COMBUSTION PRODUCTS

4. DESCRIPTIVE NOTES (Type of report and inclusive dates)
Scientific Interim

5. AUTHOR(S) (First name, middle initial, last name)
FREDERICK P. BOYNTON
EDWARD R. FISHER

6. REPORT DATE
July 1971

7a. TOTAL NO. OF PAGES
33

7b. NO. OF REFS
13

8a. CONTRACT OR GRANT NO. ARPA Order No. 1856
F19628-72-C-0007

b. PROJECT NO., Task, Work Unit Nos.
8692 n/a n/a

c. DoD Element 62301D

d. DoD Subelement n/a

9a. ORIGINATOR'S REPORT NUMBER(S)
RIES 71-32
Special Report

9b. OTHER REPORT NO(S) (Any other numbers that may be assigned this report)
AFCRL-72-0256

10. DISTRIBUTION STATEMENT
A-Approved for public release; distribution unlimited.

11. SUPPLEMENTARY NOTES
TECH, OTHER

12. SPONSORING MILITARY ACTIVITY
Air Force Cambridge Research Laboratories
L.G. Hanscom Field
Bedford, Massachusetts 01730

13. ABSTRACT

This report presents the results of an analysis of the vibrational relaxation of a combustion gas mixture in an expanding core flow field of both a conical and contoured nozzle.

The species considered are CO, H_2, CO_2, and H_2O while the vibrational excitation is characterized through the species CO(v=1), H_2(v=1), $CO_2(\nu_3)$, $CO_2(\nu_2)$, $H_2O(\nu_3)$ and $H_2O(\nu_2)$.

It is found in this analysis that the vibrational modes of the diatomics effectively freeze at the nozzle exit conditions, the ν_2 modes of the polyatomics stay close to equilibrium with the decreasing kinetic temperature while the ν_3 modes freeze at intermediate values between the exit temperature and the decreasing kinetic temperature.

The sensitivity of the vibrational relaxation to the assumed rate coefficients is discussed together with the influence of downstream shock structure.

DD FORM 1 NOV 65 1473

UNCLASSIFIED
Security Classification

14. KEY WORDS	LINK A		LINK B		LINK C	
	ROLE	WT	ROLE	WT	ROLE	WT
VIBRATIONAL RELAXATION						
EXPANDING GAS FLOW						
COMBUSTION KINETICS						

Table of Contents

Introduction

In this report we investigate the extent to which the vibrational modes of a system of combustion effluents consisting of H_2, CO, CO_2, and H_2O, maintain equilibrium vibrational distributions in an expanding flow field. In describing the vibrational relaxation, only the first vibrational levels of H_2 and CO and the ν_2 (bending) and ν_3 (asymmetric stretching) modes of H_2O and CO_2 are included. This precludes any quantitative characterization of non-Boltzmann vibrational distributions such as are expected in other expansion flows[1,2] but a discussion of their possible effects is presented. In addition, the symmetric stretching modes of the polyatomic species are not explicitely included primarily due to a lack of sufficient rate coefficient data to make their inclusion meaningful.

The expansion into vacuum of flows from two different nozzles is considered in this report. The first nozzle is conical and no strong external shocks are present. The second is contoured, and a strong nozzle-induced shock system is present in this external flow. The second nozzle also operates at considerably higher mass flow than the first. The effect of vibrational relaxation on the flow enthalpy has not been included in these calculations. Since significant vibrational freezing has been predicted by these calculations the results must be viewed as qualitative particularly in the outermost streamlines. However, since many of the important vibrational rate coefficients are not well-known, particularly the vibration-vibration exchange rate coefficients involving polyatomic species, the additional uncertainty in the calculation introduced by the

uncoupled relaxation treatment is probably small.

The expanding flow fields are discussed in Section I. In Section II, the details of the relaxation chemistry included in this calculation are presented together with the rate coefficients. In Section III, the relaxation profiles are presented and the results discussed. The major conclusions of this analysis are presented in Section IV.

Fluid Mechanical Calculations

Because the temperatures and densities within the nozzles examined in these calculations are high, we expect significant vibrational lag only in the external flow fields. We therefore assume that the flows are in local thermodynamic equilibrium at the nozzle exit, and use the nozzle exit as the initial station in our calculations. Upon leaving the nozzle, the gases continue to expand in a pattern which depends upon the flow properties and the exit conditions, which in turn depend upon the nozzle shape. This expansion continues until the force exerted upon th anding gases by the surrounding medium balance those ch the gas exerts on this ambient fluid. Near this region a shock structure develops; in order to avoid the complications introduced by this interaction, we assume that the expansion is into a vacuum.

We also assume that finite-rate relaxation processes have a negligible effect upon the thermodynamic properties of the expanding gases. This assumption is not supported by our results. However, it has the great virtue of allowing us to decouple the relaxation from the equations of motion, and therefore makes the total calculation much simpler. In addition, it does not affect the qualitative features of the relaxation calculation. We have calculated the flow field assuming local thermodynamic equilibrium everywhere. Vibrational lag would result in a somewhat lower temperature at a given density, and in a slightly different pattern of expansion, and therefore an enhanced tendency to "freeze" the vibrational populations at a somewhat earlier time.

Fluid Mechanical Calculations

Because the temperatures and densities within the nozzles examined in these calculations are high, we expect significant vibrational lag only in the external flow fields. We therefore assume that the flows are in local thermodynamic equilibrium at the nozzle exit, and use the nozzle exit as the initial station in our calculations. Upon leaving the nozzle, the gases continue to expand in a pattern which depends upon the flow properties and the exit conditions, which in turn depend upon the nozzle shape. This expansion continues until the force exerted upon the expanding gases by the surrounding medium balance those which the gas exerts on this ambient fluid. Near this region a shock structure develops; in order to avoid the complications introduced by this interaction, we assume that the expansion is into a vacuum.

We also assume that finite-rate relaxation processes have a negligible effect upon the thermodynamic properties of the expanding gases. This assumption is not supported by our results. However, it has the great virtue of allowing us to decouple the relaxation from the equations of motion, and therefore makes the total calculation much simpler. In addition, it does not affect the qualitative features of the relaxation calculation. We have calculated the flow field assuming local thermodynamic equilibrium everywhere. Vibrational lag would result in a somewhat lower temperature at a given density, and in a slightly different pattern of expansion, and therefore an enhanced tendency to "freeze" the vibrational populations at a somewhat earlier time.

Two separate nozzle flow fields have been examined in these calculations (See Figures 1a and 1b). Both burn hydrocarbon fuels with oxygen, under fuel-rich conditions, and the major product species are H_2, H_2O, CO, and CO_2.

The first nozzle is conical (15° half-angle); the flow rate is approximately 4 kgm/sec., with an assumed exhaust composition in mole per cent of 28.3% H_2, 21.7% H_2O, 42.7% CO, and 7.2% CO_2. We assume that conditions are homogeneous and source-like at the nozzle exit plane, where the temperature and pressure are $1550^\circ K$ and 0.68 atm. The expansion of this flow is calculated with the aid of a finite difference computer program[3] allowing for variable specific heats. The flow field is shown in Figure 1a which presents isotherm in the external field and also shows the streamlines along which the relaxation calculations were performed. Temperature histories along these streamlines are shown in Figure 2. We should note that the presence of a wall boundary layer in the nozzle would have a significant effect upon the flow at large angles as well as on the gas properties in this region. We have not included these effects in our calculations.

The second nozzle is larger than the first and incorporates a number of additional features. The nozzle is contoured, with the result that at the exit plane the pressure near the wall is considerably higher than at the nozzle centerline. This pressure difference causes a shock system to form in the external field. (This shock system is produced by the nozzle, and is separate from the shock system which develops as the expanding flow encounters the ambient medium. The nozzle shock system is present even in the flow into a vacuum.) The shock created as the wall gases expand into the central gases is irregularly reflected from the axis, with the formation of a Mach disc. We also allow for a

Figure 1a: Core flow field for a conical nozzle expanding into a vacuum.

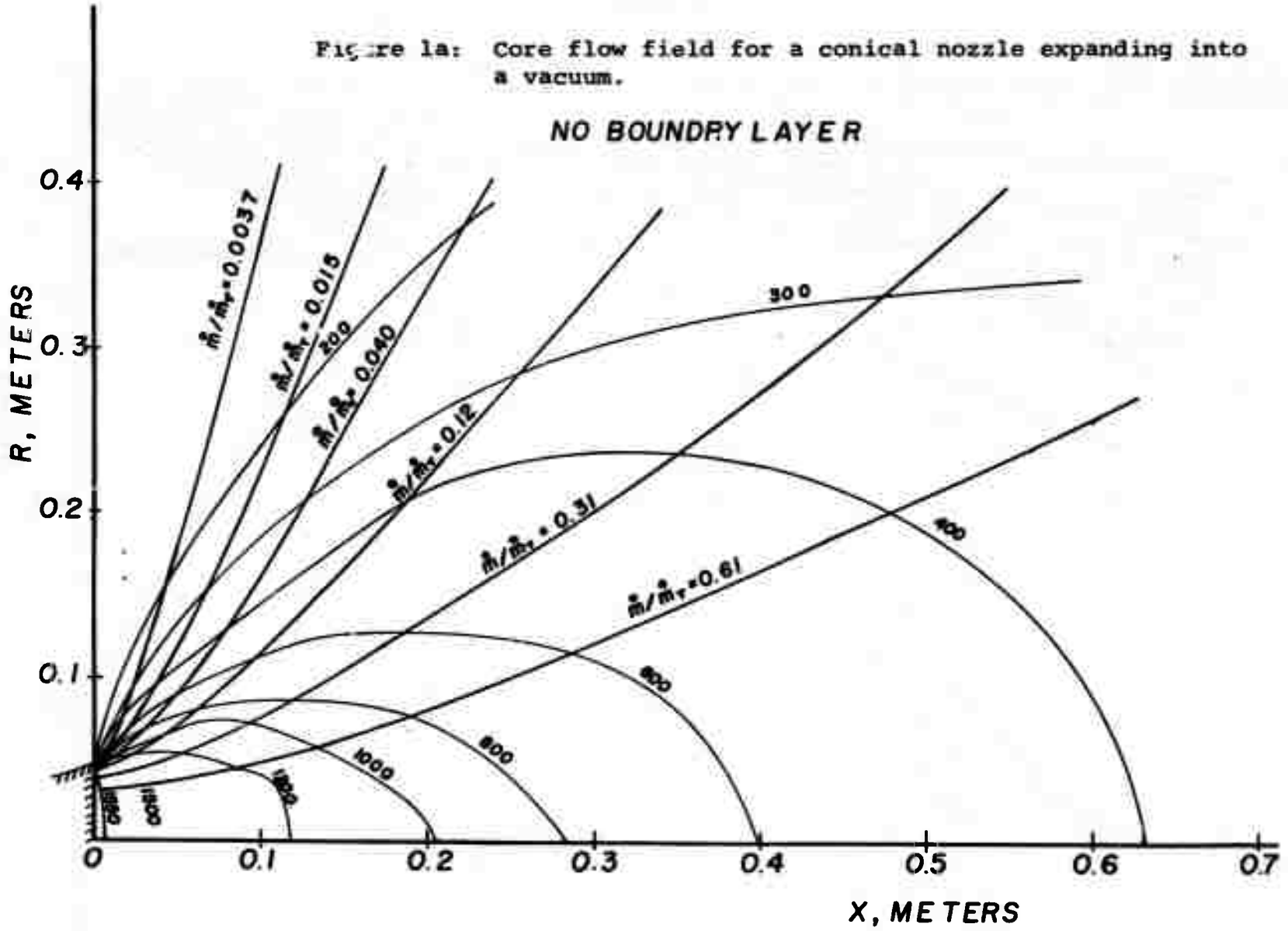

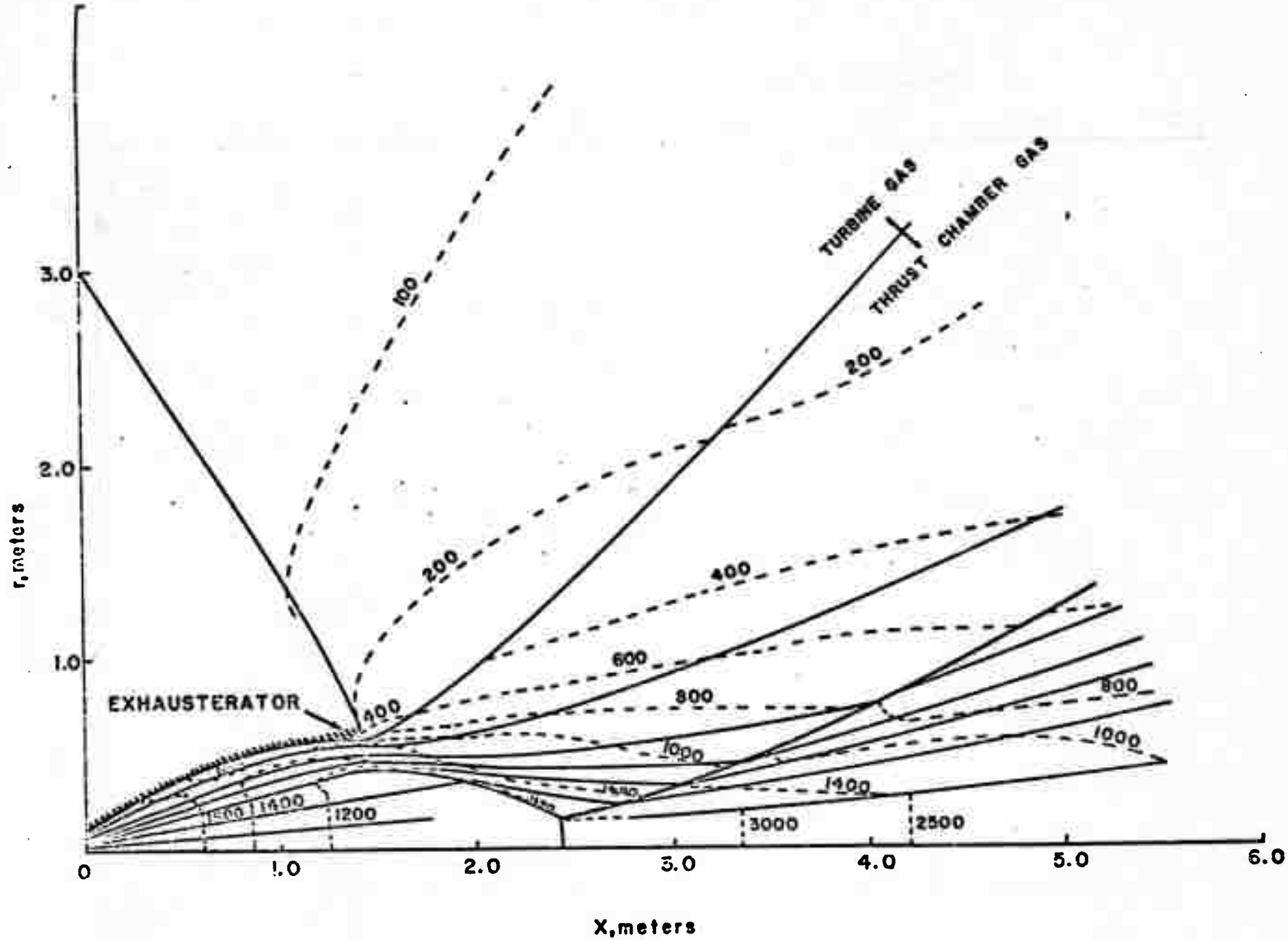

Figure 1b: Core flow field for a contoured nozzle expanding into a vacuum.

Figure 2: Temperature - time histories along various streamlines for the conical nozzle flow field shown in Figure 1a.

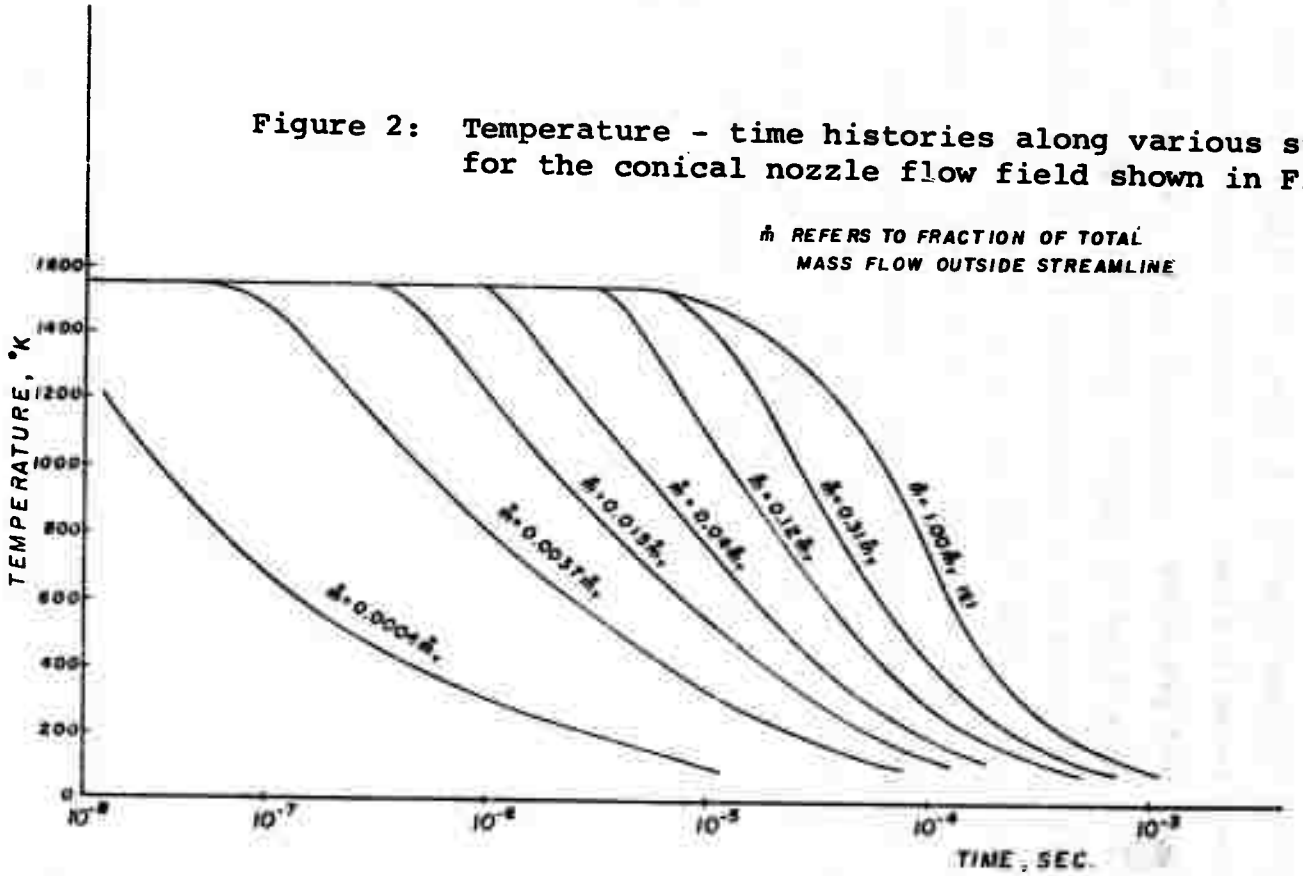

variation in flow composition normal to the streamlines. (It is a common practice in nozzle design to provide a fuel-rich layer near the wall to reduce thermal loads on the structure. Furthermore, we allow for the presence of an annular shroud of gases of different compostion from the main flow. This ducted gas confines the main flow, and prevents its expanding to larger angles. The total main flow is approximately 115 kgm/sec. The flow field is again calculated using the finite-difference procedure. (The calculation is discussed in detail in Ref. 4). The external field is shown in Figure 16. Temperature histories along these streamlines are shown in Figure 3. Note the shock structure and its effect on the temperature field downstream of the shocks; we shall see that this has an effect upon relaxation along streamlines passing through the shock system.

Figure 3: Temperature - time histories along various streamlines for the contoured nozzle flow field shown in Figure 1b.

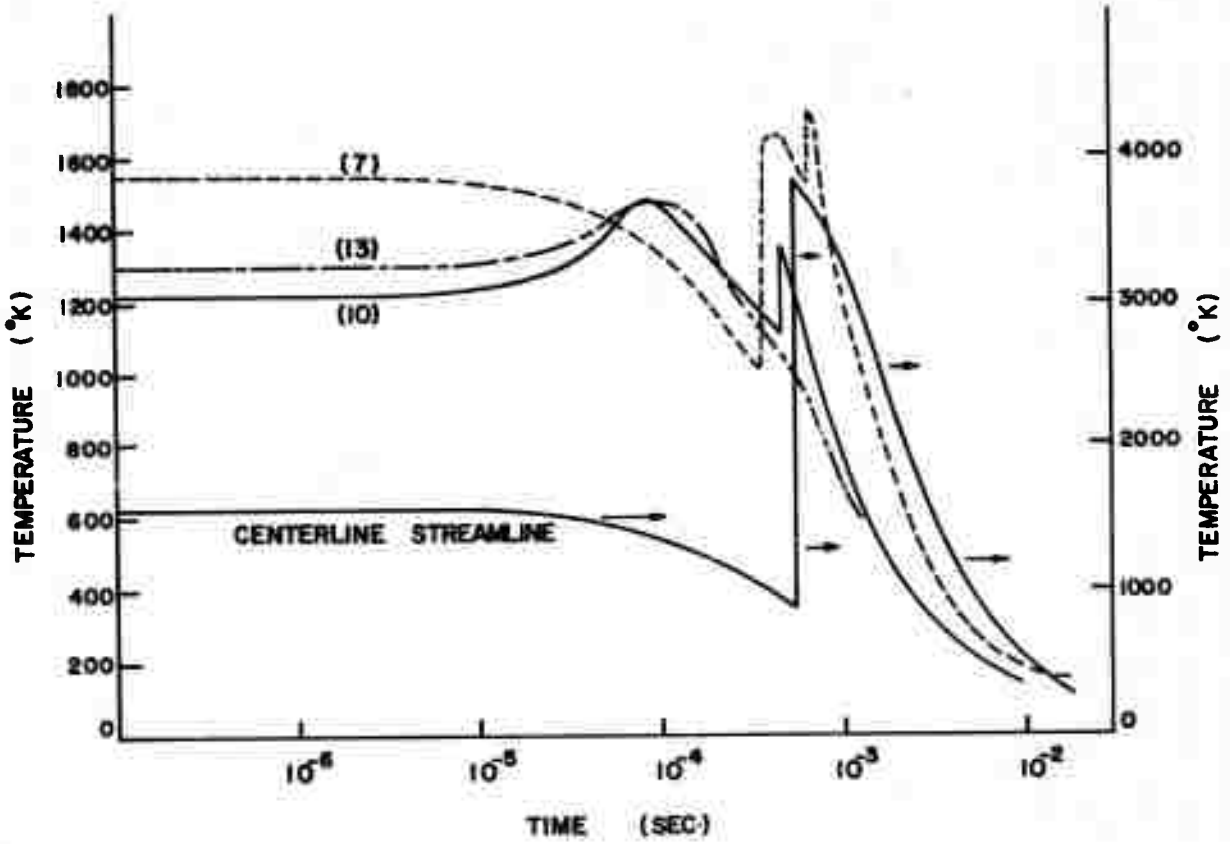

Vibrational Relaxation Chemistry

In this section, the specific excitation processes and rate coefficients used in these relaxation studies are presented. The extent of equilibration of the vibrational modes with the translational temperature as given in Figures 2 and 3, is calculated for the species CO, H_2, CO_2 and H_2O. Only the first vibrational level is included for the diatomics and the symmetric stretch modes of the triatomics are not explicitely included due to lack of sufficient rate coefficient data to make their inclusion meaningful. By not including the higher vibrational levels in this treatment, the possibility of characterizing the non-Boltzmann character in the vibrational distributions is eliminated[5]. However, the major purpose of these calculations is to estimate the extent of deviation of the vibrational levels from equilibration with the translational temperature during an expansion to vacuum. We express the results in the form of effective vibrational temperatures through the equation

$$n(1) = n(o) \exp\{-E_{10}/kT_v\} \tag{1}$$

where n(1) and n(o) are the upper state and ground state species densities, respectively, E_{10} is the vibrational energy level spacing and T_v is the effective vibrational temperature. The actual vibrational structure and the appropriate energy spacing is shown in Table I.

Vibrational relaxation of exhaust species will occur through both vibration-translation (VT) and vibration-vibration (VV) energy transfer processes. In general, VV processes are rapid compared to VT processes for temperatures below about 1000°K. Thus, some vibrational modes with relatively slow VT

TABLE I

COMBUSTION SPECIES AND SPECTROSCOPIC PARAMETERS

SPECIES	ENERGY ABOVE GROUND
$CO(\nu = 1)$	2143 cm^{-1}
$CO(\nu = 0)$	
$H_2(\nu = 1)$	4161 cm^{-1}
$H_2(\nu = 0)$	
$CO_2(\nu = \nu_3)$	2349 cm^{-1}
$CO_2(\nu = \nu_2)$	667 cm^{-1}
$CO_2(\nu = 0)$	
$H_2O(\nu = \nu_3)$	3755 cm^{-1}
$H_2O(\nu = \nu_2)$	1595 cm^{-1}
$H_2O(\nu = 0)$	

TABLE II

RELAXATION REACTIONS AND RATE COEFFICIENTS

	REACTION		RATE COEFFICIENT
	VIBRATION-TRANSLATION REACTIONS		
1.	$CO(v=1) + H_2 \rightleftarrows CO(v=0) + H_2$	(1)	$\ell n(p\tau) = (68/T^{\frac{1}{3}}) - 19.59$
2.	$CO(v=1) + CO_2 \rightleftarrows CO(v=0) + CO_2$	(2)	$\ell n(p\tau) = (241.16/T^{\frac{1}{3}}) - 33.37$
3.	$CO(v=1) + H_2O \rightleftarrows CO(v=0) + H_2O$	(1)	$6.7^{-15}\exp[2.5^{-3}T]$
4.	$H_2(v=1) + H_2 \rightleftarrows H_2(v=0) + H_2$	(3)	$p\tau = 3.9^{-10}\exp[100/T^{\frac{1}{3}}]$
5.	$H_2(v=1) + CO_2 \rightleftarrows H_2(v=0) + CO_2$	(2)	$\ell n(p\tau) = (174.61/T^{\frac{1}{3}}) - 21.49$
6.	$H_2(v=1) + H_2O \rightleftarrows H_2(v=0) + H_2O$	(2)	$\ell n(p\tau) = (169.37/T^{\frac{1}{3}}) - 21.37$
7.	$CO_2(v=\nu_3) + H_2 \rightleftarrows CO_2(v=0) + H_2$	(2)	$\ell n(p\tau) = (81.47/T^{\frac{1}{3}}) - 19.85$
8.	$CO_2(v=\nu_3) + CO_2 \rightleftarrows CO_2(v=0) + CO_2$	(2)	$\ell n(p\tau) = (276.27/T^{\frac{1}{3}}) - 27.40$
9.	$CO_2(v=\nu_3) + H_2O \rightleftarrows CO_2(v=0) + H_2O$	(2)	$\ell n(p\tau) = (210.52/T^{\frac{1}{3}}) - 24.40$
10.	$CO_2(v=\nu_2) + H_2 \rightleftarrows CO_2(v=0) + H_2$	(1)	$3.56^{-12}\exp[-8.04^{-4}T]$
11.	$CO_2(v=\nu_2) + CO_2 \rightleftarrows CO_2(v=0) + CO_2$	(1)	$5.9^{-22}T^{2.77}$
12.	$CO_2(v=\nu_2) + H_2O \rightleftarrows CO_2(v=0) + H_2O$	(1)	$3.95^{-11}\exp[-3.23^{-3}T]$
13.	$H_2O(v=\nu_3) + H_2 \rightleftarrows H_2O(v=0) + H_2$	(2)	$\ell n(p\tau) = (147.7/T^{\frac{1}{3}}) - 20.99$
14.	$H_2O(v=\nu_3) + CO_2 \rightleftarrows H_2O(v=0) + CO_2$	(2)	$\ell n(p\tau) = (393.48/T^{\frac{1}{3}}) - 29.59$
15.	$H_2O(v=\nu_3) + H_2O \rightleftarrows H_2O(v=0) + H_2O$	(2)	$\ell n(p\tau) = (330.28/T^{\frac{1}{3}}) - 27.01$
16.	$H_2O(v=\nu_2) + H_2 \rightleftarrows H_2O(v=0) + H_2$	(2)	$\ell n(p\tau) = (47.16/T^{\frac{1}{3}}) - 19.24$
17.	$H_2O(v=\nu_2) + CO_2 \rightleftarrows H_2O(v=0) + CO_2$	(2)	$\ell n(p\tau) = (125.64/T^{\frac{1}{3}}) - 21.99$
18.	$H_2O(v=\nu_2) + H_2O \rightleftarrows H_2O(v=0) + H_2O$	(1)	$8.74^{-12} + 9.36^{-9}/T$
19.	$CO_2(v=\nu_3) + H_2 \rightleftarrows CO_2(v=\nu_2) + H_2$	(1)	4^{-14}
20.	$CO_2(v=\nu_3) + CO_2 \rightleftarrows CO_2(v=\nu_2) + CO_2$	(1)	$3.58^{-14} + 9.43^{-17}T$
21.	$CO_2(v=\nu_3) + H_2O \rightleftarrows CO_2(v=\nu_2) + H_2O$	(1)	$5.47^{-13} - 3.03^{-16}T$
22.	$H_2O(v=\nu_3) + H_2 \rightleftarrows H_2O(v=\nu_2) + H_2$	(2)	$\ell n(p\tau) = (70.66/T^{\frac{1}{3}}) - 19.34$
23.	$H_2O(v=\nu_3) + CO_2 \rightleftarrows H_2O(v=\nu_2) + CO_2$	(2)	$\ell n(p\tau) = (188.24/T^{\frac{1}{3}}) - 23.76$
24.	$H_2O(v=\nu_3) + H_2O \rightleftarrows H_2O(v=\nu_2) + H_2O$	(2)	$\ell n(p\tau) = (158/T^{\frac{1}{3}}) - 22.53$

TABLE II continued

	VIBRATION-VIBRATION REACTIONS		RATE COEFFICIENT
25.	$H_2(v=1) + CO(v=0) \rightleftarrows H_2(v=0) + CO(v=1)$	(4)	$3.77^{-13} T^{5/6} \exp[-88.7/T^{\frac{1}{3}}]$
26.	$CO_2(v=v_3) + CO(v=0) \rightleftarrows CO_2(v=0) + CO(v=1)$	(4)	$2^{-14} T^{5/6} \exp[-36.55/T^{\frac{1}{3}}]$
27.	$H_2O(v=v_3) + CO(v=0) \rightleftarrows H_2O(v=0) + CO(v=1)$	(4)	$3.22^{-13} T^{5/6} \exp[-136.1/T^{\frac{1}{3}}]$
28.	$H_2(v=1) + H_2O(v=0) \rightleftarrows H_2(v=0) + H_2O(v=v_3)$	(4)	$4.11^{-14} T^{5/6} \exp[-31.5/T^{\frac{1}{3}}]$
29.	$CO_2(v=v_3) + H_2O(v=0) \rightleftarrows CO_2(v=v_2) + H_2O(v=v_2)$	(4)	$2.17^{-14} T^{5/6} \exp[-23.87/T^{\frac{1}{3}}]$
30.	$H_2O(v=v_3) + CO(v=0) \rightleftarrows H_2O(v=v_2) + CO(v=1)$	(4)	$1.34^{-15} T^{5/6} \exp[-6.68/T^{\frac{1}{3}}]$
31.	$CO_2(v=v_3) + H_2O(v=v_2) \rightleftarrows CO_2(v=0) + H_2O(v=v_3)$	(4)	$1.9^{-14} T^{5/6} \exp[-30.96/T^{\frac{1}{3}}]$

will preferentially relax by transfering energy to molecules with faster VT rates through VV coupling. Although only a partial set of vibrational levels have been included in these calculations, an attempt has been made to include all the important transfer processes which affect these levels. A list of the relaxation processes included is given in Table II together with the adopted rate coefficient. Since several of the necessary rate coefficients are unknown, they have been estimated by using Millikan and White's[6] correlation for VT processes and from the modified Rapp-Englander Golden[7] model for VV processes.

For VT rates, the anticipated relaxation time values ($p\tau$) have been converted to rate coefficients by the equation[8]

$$k = \frac{RT}{p\tau}\left[1-e^{-E_{10}/kT}\right]^{-1} \qquad (2)$$

where T is the translational temperature. No major uncertainty is expected from the use of this conversion equation although the estimated values of $p\tau$ particularly for the H_2O molecule are not expected to be very reliable. Fortunately, some new rate coefficient values are available from recent molecular laser systems[9]. These results have been included where appropriate.

The VV rates have been either taken from recent measurements of interest to laser system[9,10] or have been calculated from the following rate coefficient expressions[1,7]

(3) $$k^{rn}_{sm}\big|_{LEDL} = 1.508^{-13}\mu_M^{7/6} L_A^{10/3} \sigma_A^2 \bar{E}_d^{4/3} U^2_{rn} U^2_{sm} T^{5/6} \cdot \exp\left\{-1.32 (L_A \bar{E}_d)^{6/3} \frac{\mu_M}{T}\right\}^{1/3}$$

and

(4) $$k^{rn}_{sm}\big|_{SEDL} = 8.88^{-13} \mu_M L_A^2 \sigma_A^2 T_2^3 U^2_{rn} U^2_{sm} \left\{1 - 5.703^{-3} \frac{\mu_M L_A^2 \bar{E}_d^{-2}}{T}\right\}$$

where

μ_M = reduced mass in molecular units
L_A = exponential parameter in Å.
σ_A = hard sphere diameter in Å.
T = temperature in °K
$\bar{E}_d$ = energy defect in cm^{-1}

and

U_{rn} = matrix element for r→n vibrational transition.

The subscripts on these VV rate coefficients refer to larger energy defect limit (LEDL) and small energy defect limit (SEDL) and suggest the range of application for each equation. In general, when the difference in the vibrational quanta being exchanged is larger than about 20 cm^{-1}, equation (3) should be used. These estimated VV rate coefficients may be subject to considerable error (although probably not more than an order of magnitude in the worst case) particularly in the temperature dependence. As is well known, the temperature dependence of near resonant VV processes may become negative at temperatures below about 1000°K due to long range interactions. This has been confirmed in the N_2 - CO_2

system.[11] Unfortunately insufficient data are available to assess this possibility for other systems particularly involving H_2O. It is likely therefore that the temperature dependence as given by equations (3) and (4) will not be correct for very near resonant VV processes considered here. However, it is unlikely that the qualitative features of the relaxation results would be affected.

Relaxation Results

The coupled set of relaxation equations with the appropriate rate coefficients as given in Table II have been integrated along the various streamlines shown in Figures 2 and 3, using a Runge-Kutta-Merson procedure[1,12]. The translational temperature and density were treated as known functions of time for the integration.

The Runge-Kutta-Merson integration procedure used features a variable time step consistent with equation stability and also contains an algebraic algorithm for integrating those relaxation equations which are sufficiently close to steady state to make the set of equations "stiff".[12]

Representative results for the relaxation calculation are given in Figures 4 through 8 for the conical nozzle flow and in Figures 9 through 13 for the contoured nozzle flow. As expected, the low lying bending modes of both CO_2 and H_2O show significant vibrational freezing only in the outermost streamlines for which the expansion is most rapid. The higher lying vibrational modes, particularly of the diatomics, show freezing behavior for almost all streamlines considered. For those cases where the relaxation behavior is calculated through the Mach disc, i. e. Figure 9, the flow remains in equilibrium until some distance downstream from the Mach disc due primarily to the high densities in this region of the flow.

Figure 4: Vibrational temperature history along the center streamline of the conical nozzle flow field. The assumed composition is 28.3% H_2, 21.7% H_2O, 42.7% CO and 7.2% CO_2.

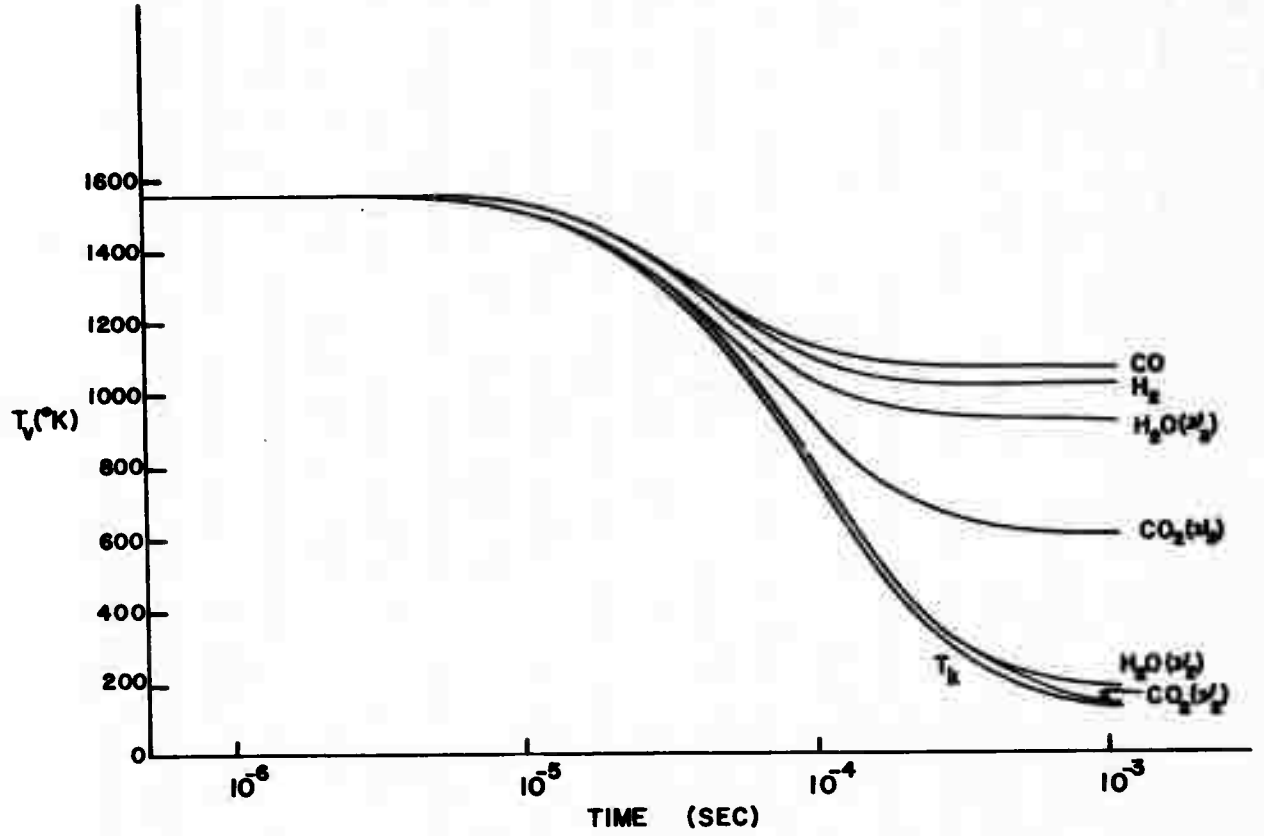

Figure 5: Vibrational temperature history along a streamline in the conical nozzle flow field for which m = 0.0394 m_t. The assumed composition is 28.3% H_2, 21.7% H_2O, 42.7% CO and 7.2% CO_2.

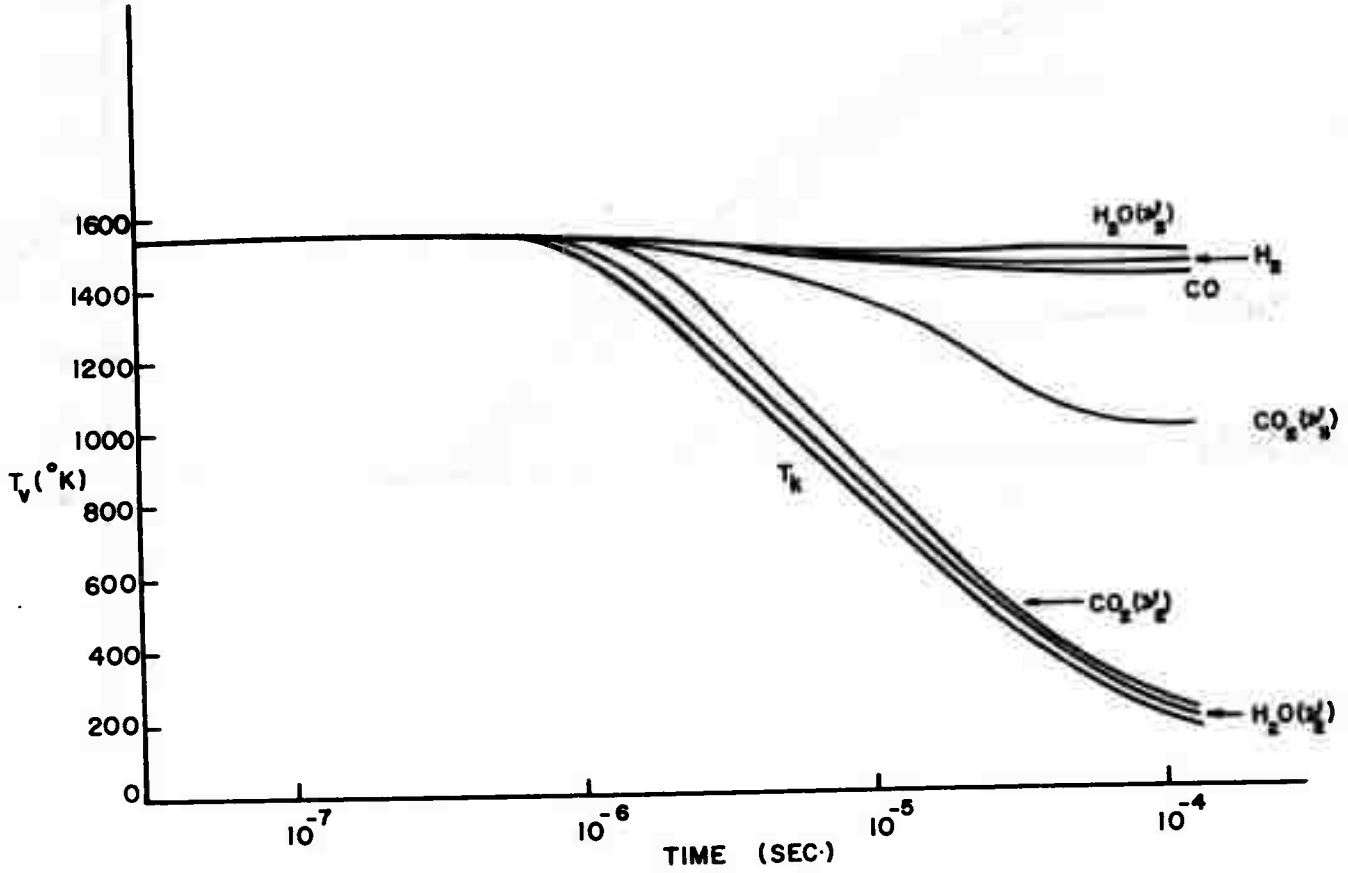

Figure 6: Vibrational temperature history along a streamline in the conical nozzle flow field for which m = 0.015 m_t. The assumed composition is 28.3% H_2, 21.7% H_2O, 42.7% CO and 7.2% CO_2.

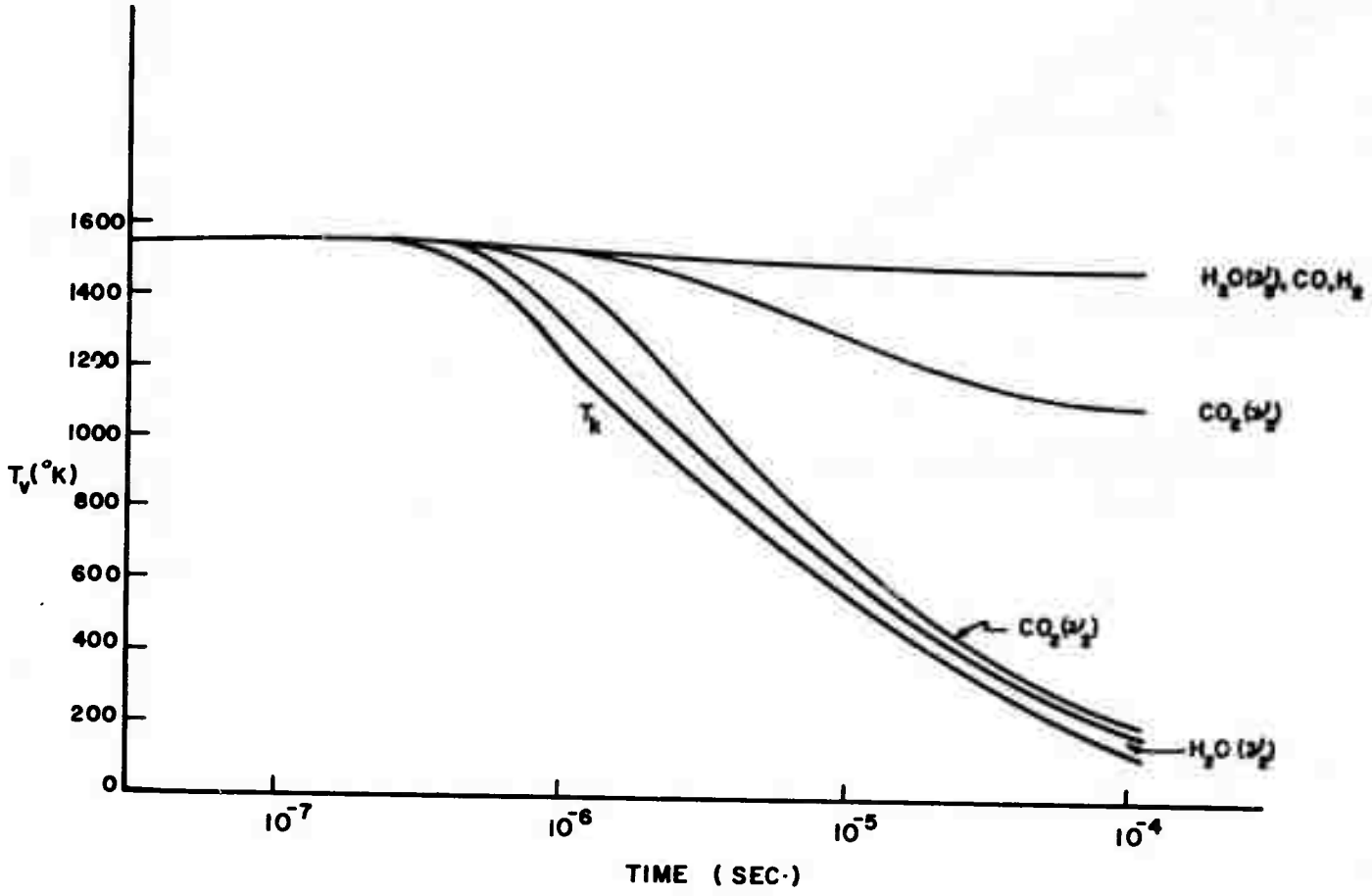

Figure 7: Vibrational temperature history along a streamline in the conical nozzle flow field for which m = 0.0037 m_t. The assumed composition is 28.3% H_2, 21.7% H_2O, 42.7% CO and 7.2% CO_2.

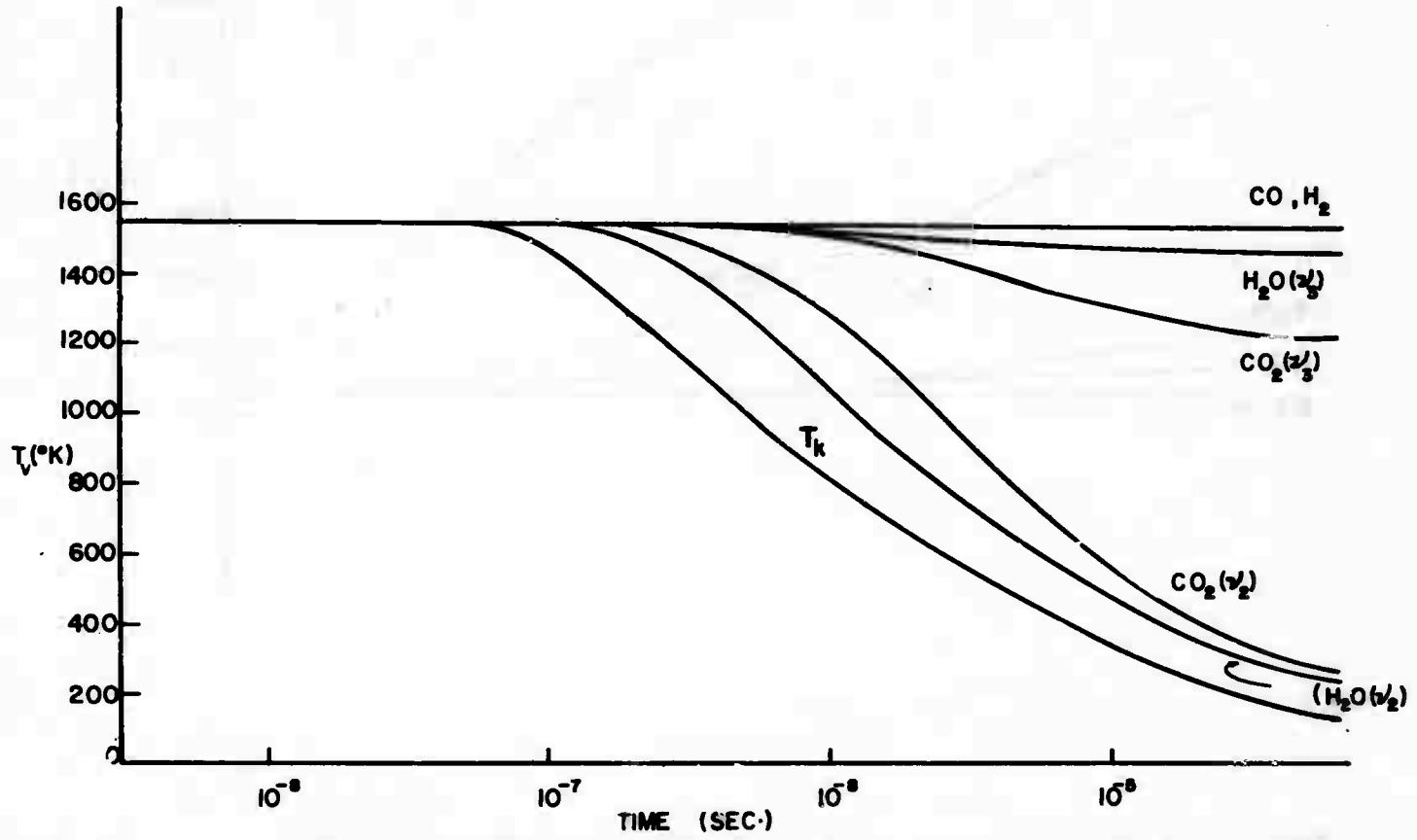

Figure 8: Vibrational temperature history along a streamline in the conical nozzle flow field for which m = 0.0004 m_t. The assumed composition is 28.3% H_2, 21.7% H_2O, 42.7% CO and 7.2% CO_2.

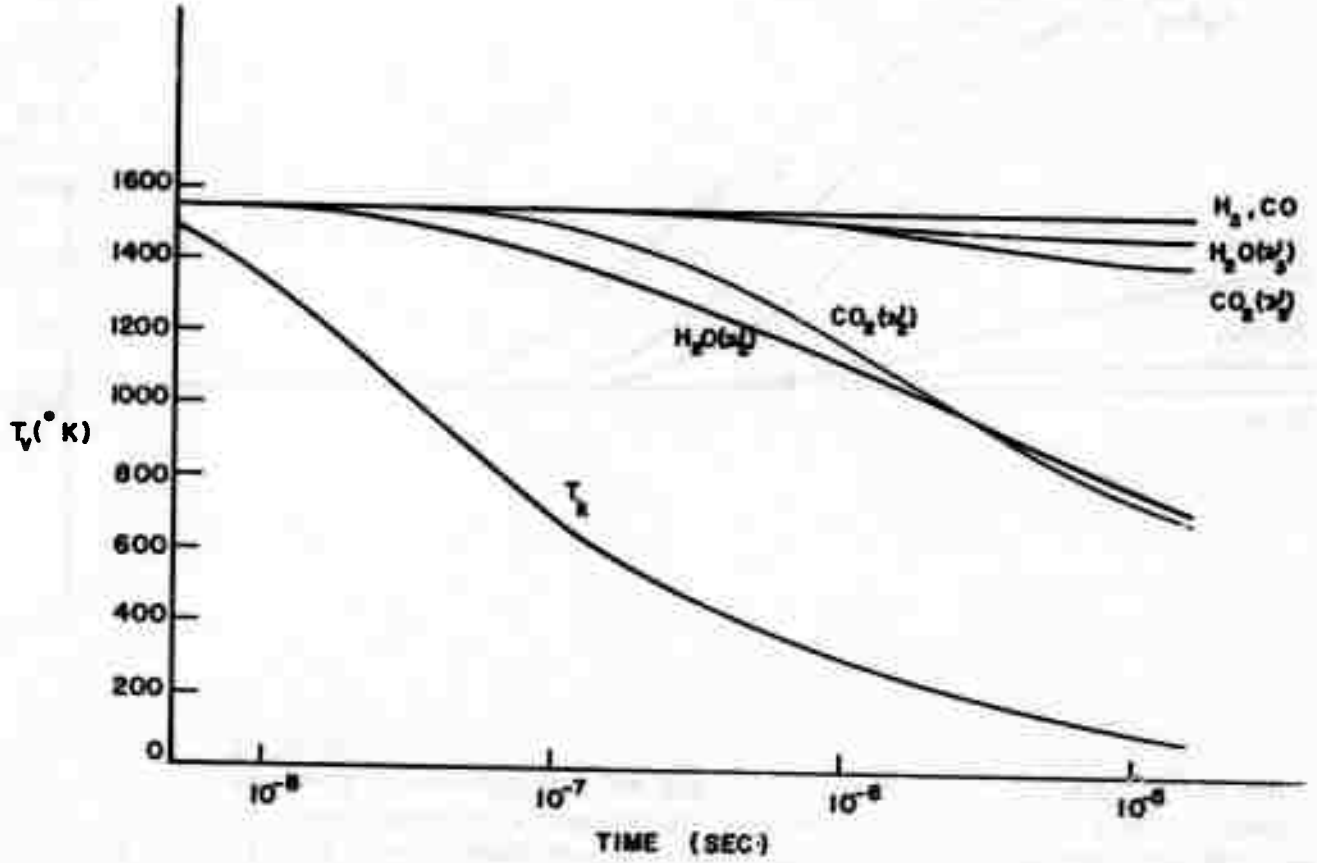

Figure 9: Vibrational temperature history along a streamline just outside the Mach disc ($m = 0.878\ m_t$) for the contoured nozzle flow field. The assumed composition is 10.3% H_2, 40.4% H_2O, 25.2% CO and 24.1% CO_2.

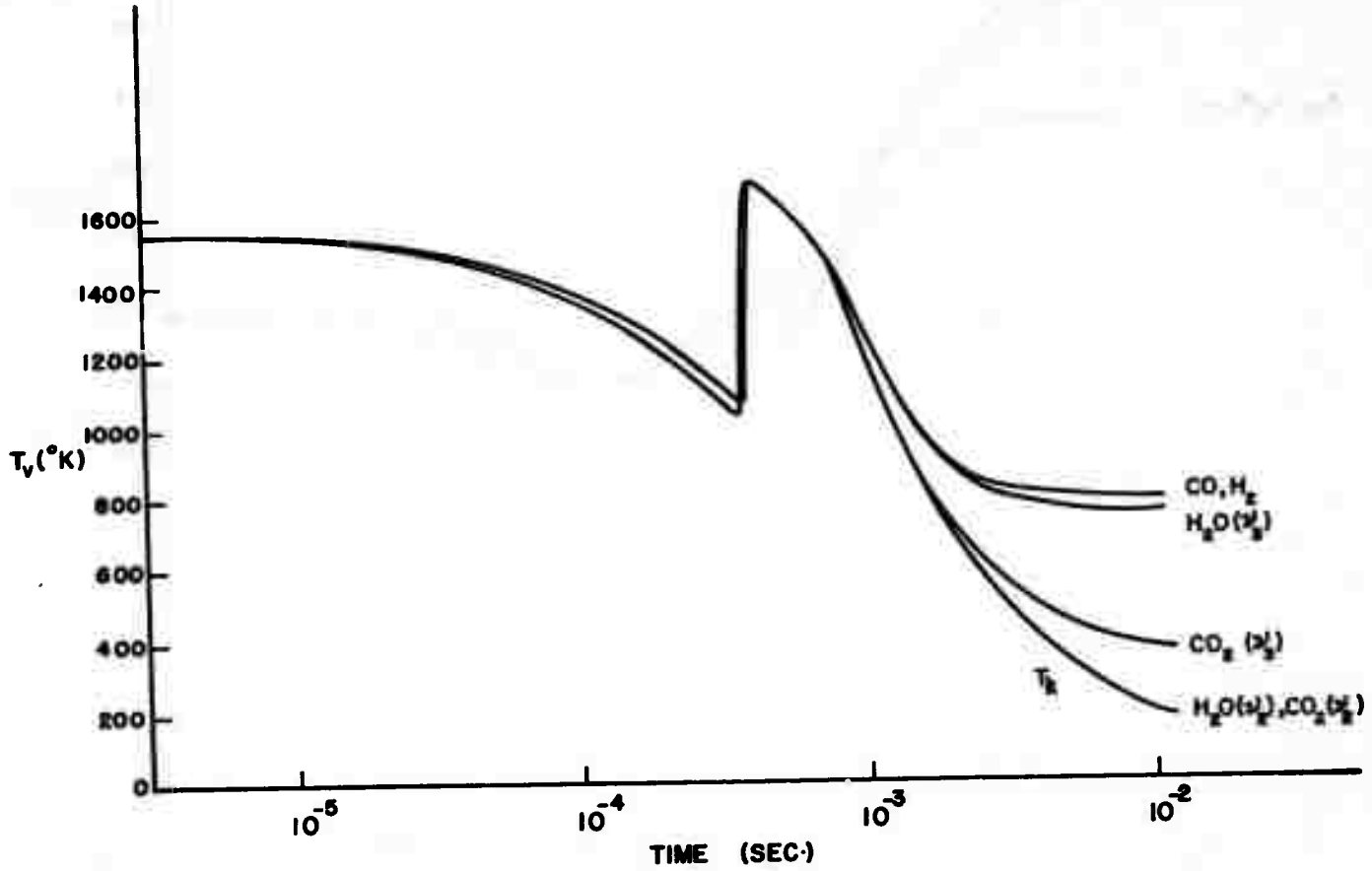

Figure 10: Vibrational temperature history along a streamline in the contoured nozzle flow field for which m = 0.784 m_t. The assumed composition is 10.3% H_2, 40.4% H_2O, 25.2% CO and 24.1% CO_2.

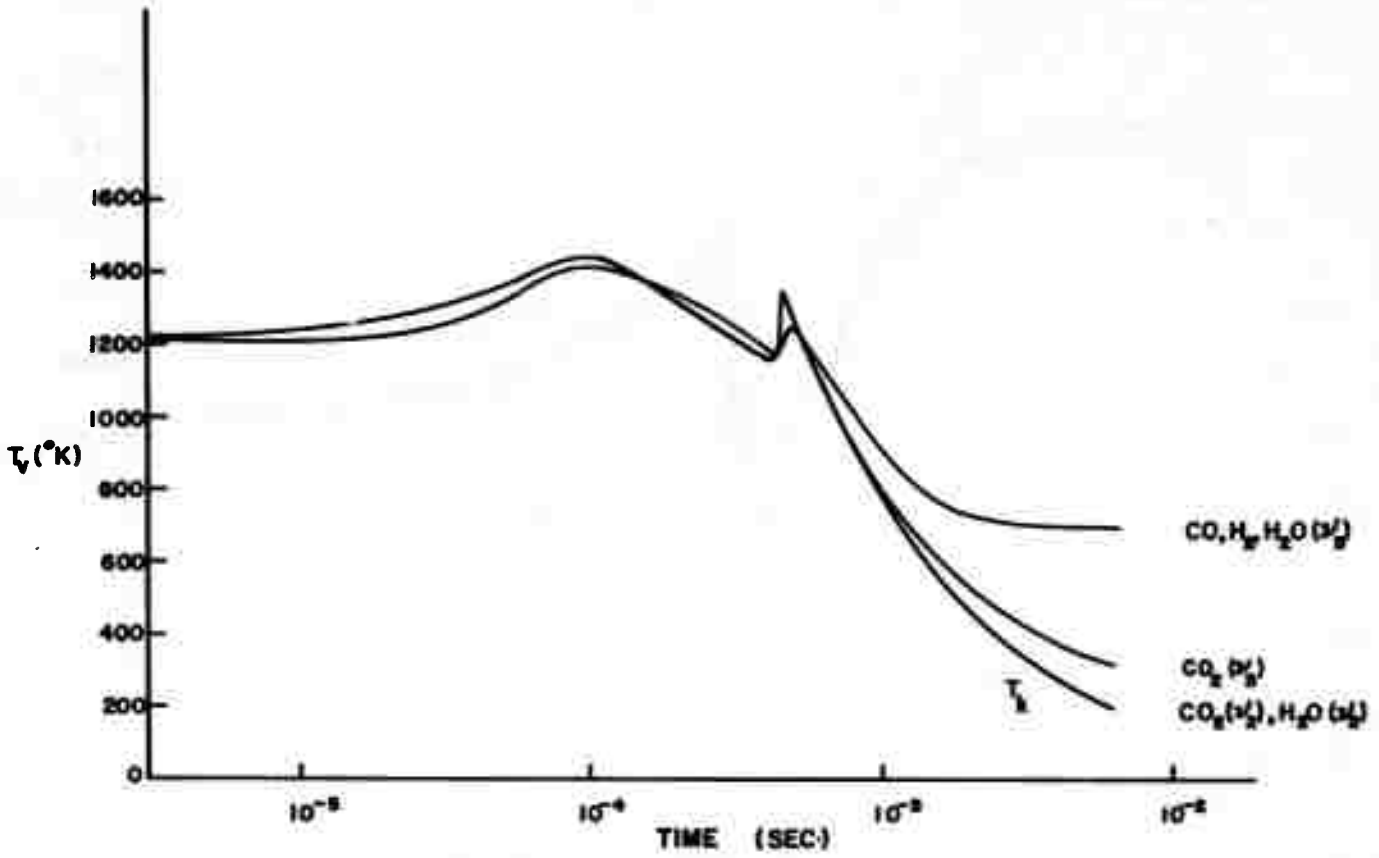

Figure 11: Vibrational temperature history along a streamline in the contoured nozzle flow field for which m = 0.663 m_t. The assumed composition is 10.3% H_2, 40.4% H_2O, 25.2% CO and 24.1% CO_2.

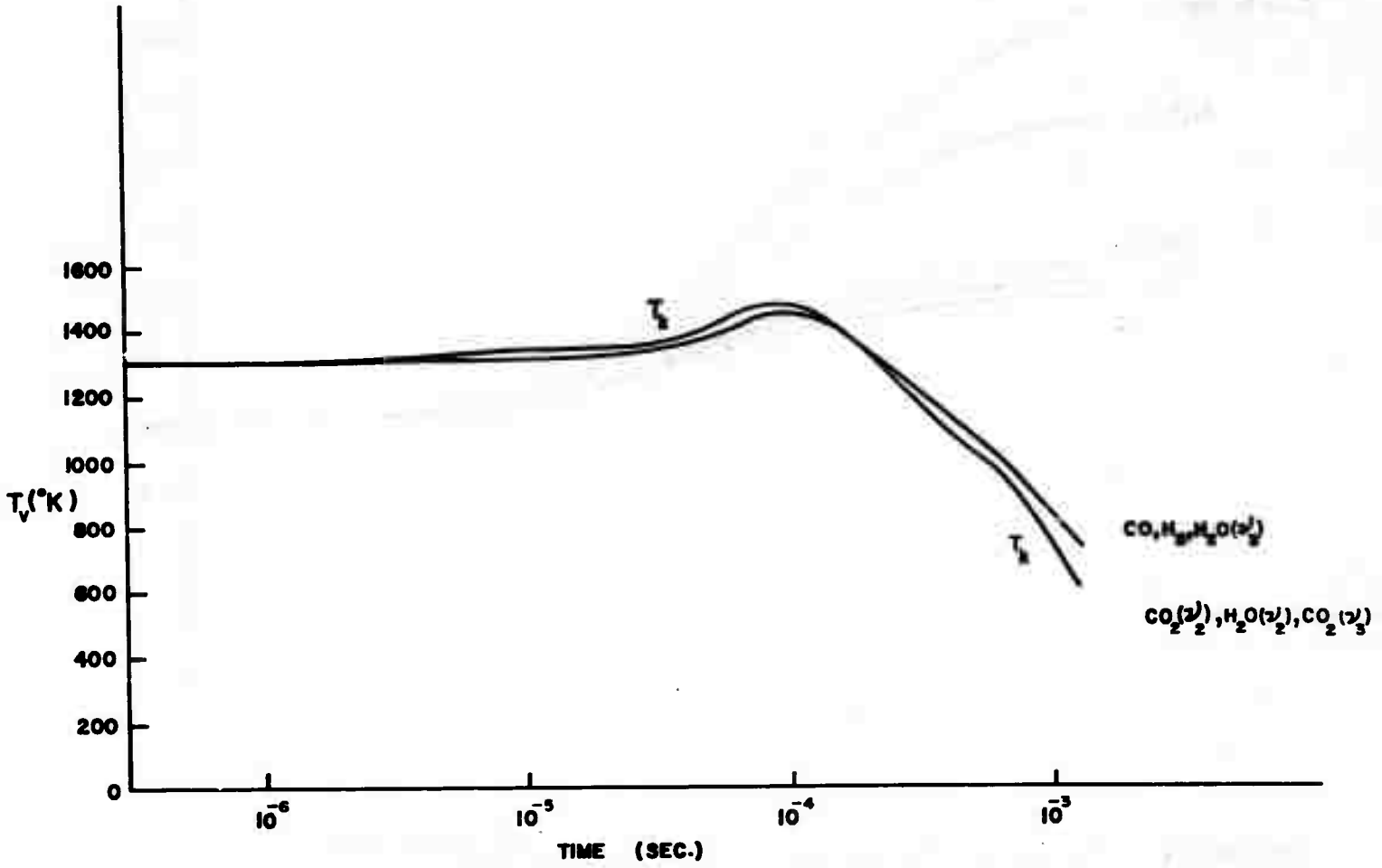

Figure 12: Vibrational temperature history along a streamline in the contoured nozzle flow field for which m = 0.325 m_t. The assumed composition is 14.8% H_2, 35.1% H_2O, 31.5% CO and 18.5% CO_2.

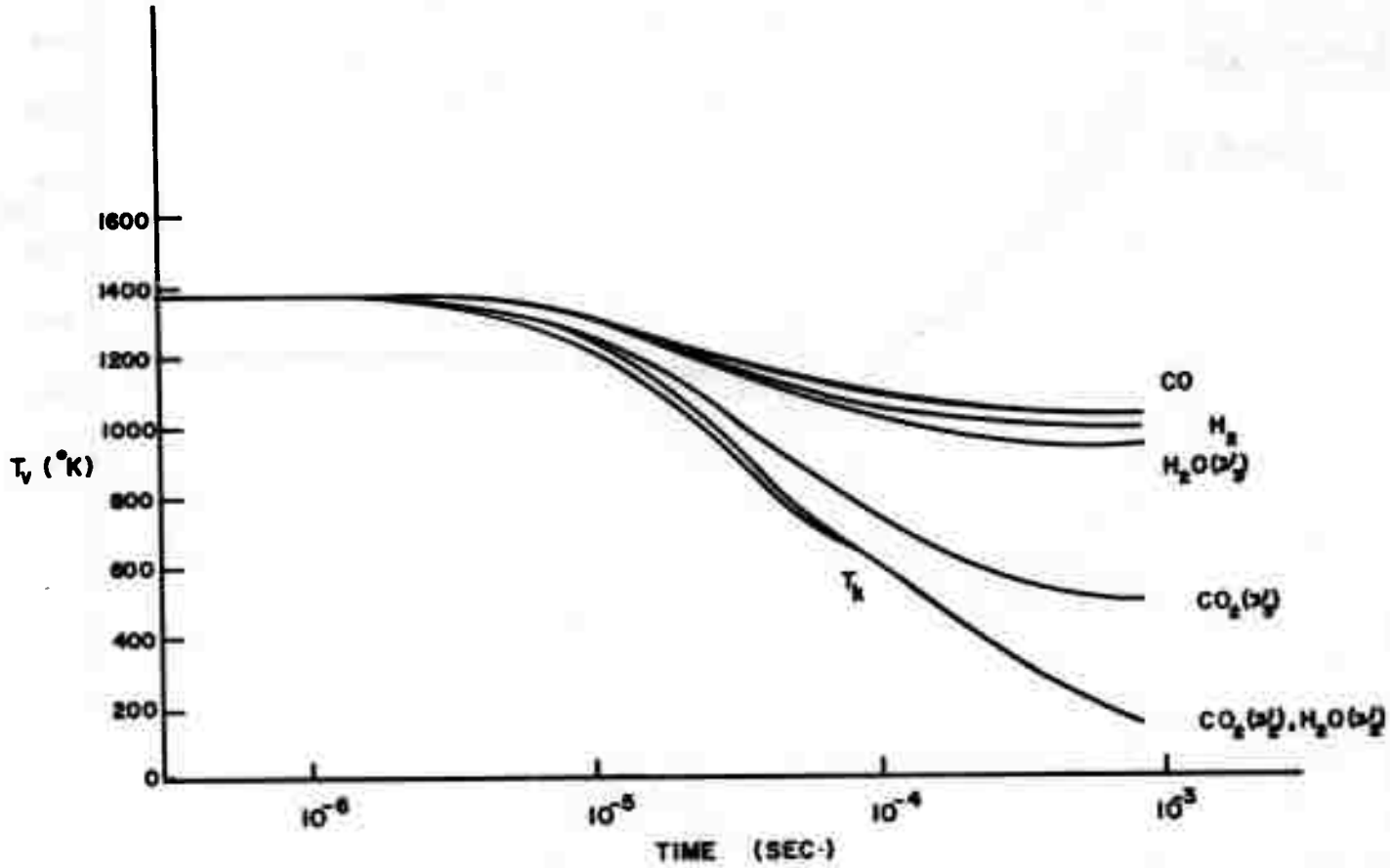

Figure 13: Vibrational temperature history along a wall streamline of the contoured nozzle flow field for which m = 0.066 m_t. The assumed composition is 23.5% H_2, 26.1% H_2O, 39.4% CO and 11.0% CO_2.

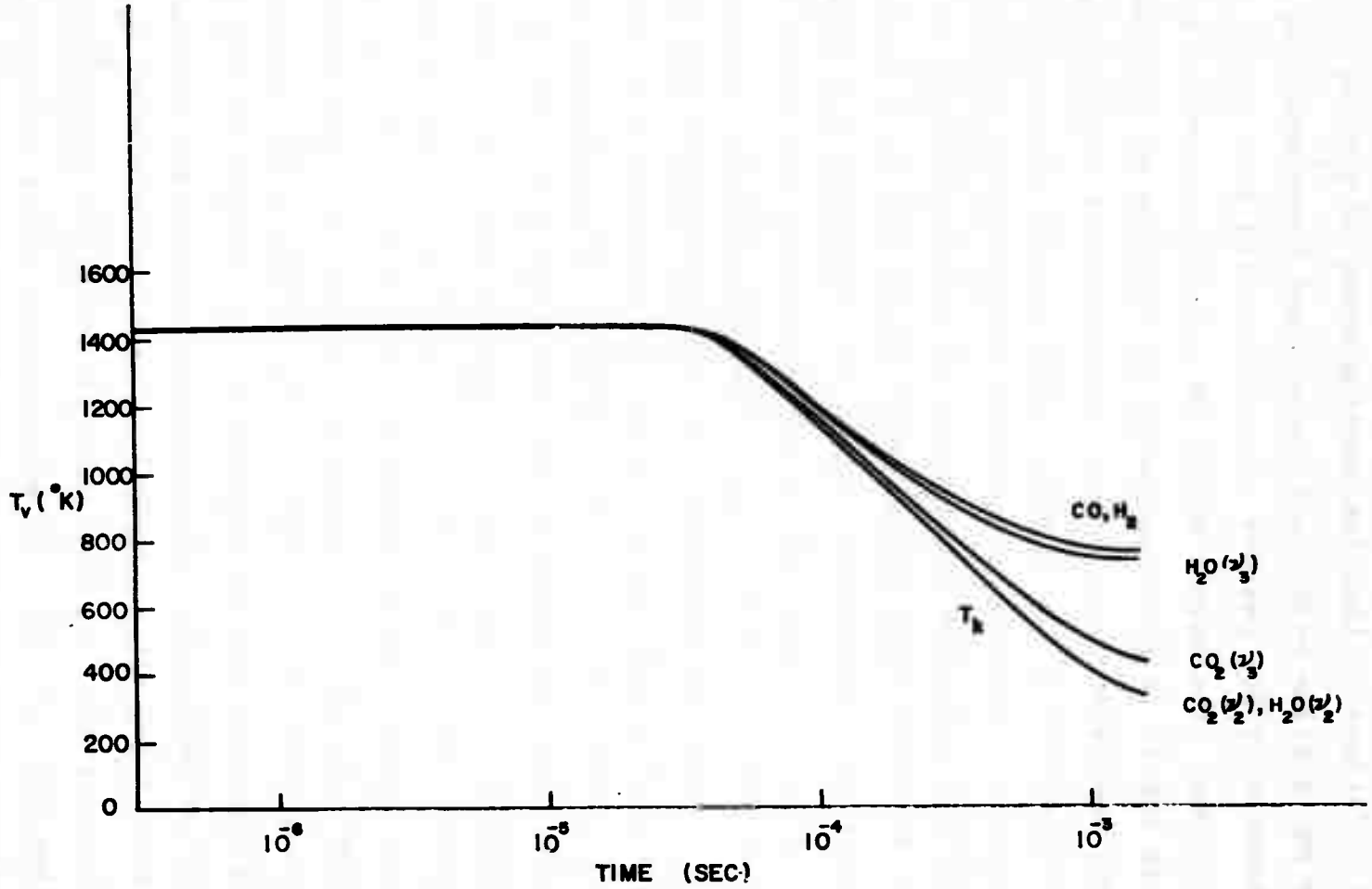

Discussion

The major conclusions to be drawn from these relaxation calculations is that the bending modes of H_2O and CO_2 are in equilibrium with the translational temperature in essentially all regions of the expanding flow except the outermost streamlines where the expansion is most rapid. This result is not expected to be affected by improved rate coefficients as enough information is available on the kinetics of the bending modes to make their modeling reliable. The stretching modes of H_2O and CO_2 and the diatomic modes are largely out of equilibrium and, in fact, the diatomic modes are normally frozen out at or near the nozzle exit conditions. Since the coupling rates between the ν_3 and ν_2 modes of CO_2 are moderately well known[9] (i.e. reactions (19) - (21)), the calculations involving the ν_3 mode are expected to be fairly reliable. The comparable rate coefficients involving the H_2O molecule (i.e. reactions (22) - (24)) are not known. However, the predicted rate coefficient for reaction (22) is of the same order as the analogous reaction involving CO_2 (reaction (19)). This appears reasonable since vibration-rotation energy transfer tends to make the H_2O molecule relax faster than CO_2 but the larger quantum being transferred in the H_2O case tends to counter balance this effect. The estimates of reactions (23) and (24) are not expected to be reliable to even an order of magnitude. This was not considered a serious problem since the concentration of H_2, H_2O, and CO_2 are all comparable, and therefore reaction (22) dominates as over either (23) or (24). No experimental rates are available on the VV processes but from analogy to known VV rate coefficients in CO_2 - N_2[9] and N_2 - CO systems[13], equations (3) and (4) are expected to give rather reliable

values at any given temperature. As indicated earlier, however, the temperature dependence for the near resonant VV processes (i.e. reactions (29) and (30) and perhaps even for reactions (26) and (31)) may be negative at low temperatures. This would favor improved coupling between the ν_2 and ν_3 modes and would suggest somewhat lower vibrational temperatures for the ν_3 mode than shown in Figures (4) through (13). Due to the rapid decay in the translational temperature and density for these vacuum expansions, it is unlikely that improved calculations would alter the qualitative features of the figures.

Finally, we note that vibrational modes remain in equilibrium with translation in passing through the normal shock (Mach disc) formed by the contoured nozzle. However, in the re-expansion downstream from the Mach disc, significant departure from equilibrium is found. This departure will be greater for smaller nozzles, where the expansion is more rapid.

In conclusion, our calculations show appreciable vibrational freezing of combustion effluents particularly in the outermost streamlines of both the conical and contoured nozzle flow fields. This conclusion is not expected to be altered by improved rate coefficients although quantiative results will vary as both VV and VT processes are more accurately determined for those reactions involving H_2O. Due to the predicted high vibrational populations and the low translational temperatures, non-Boltzmann vibrational distributions should be evident as a result of anharmonic VV pumping [1,2].

Bibliography

(1) E.R. Fisher and R.H. Kummler, J. Chem. Phys. 49, 1075, 1085 (1968).

(2) C.E. Treanor, J.W. Rich and R.G. Rehm, J. Chem. Phys., 48, 1798 (1968).

(3) F.P. Boynton and A. Thomson, J. Computational Phys. 3, 379 (1969).

(4) F.P. Boynton, Research Institute for Engineering Sciences Report 70-18, Wayne State University (1970).

(5) It has been established particularly through molecular laser studies, that the upper vibrational levels are preferentially pumped by the lower vibrational levels due to anharmonic VV exchange processes in environments where the vibrational population is considerable higher than given by a Boltzmann equilibrium with the translational temperature.

(6) R.C. Millikan and D.R. White, J. Chem. Phys. 39, 3209 (1963).

(7) D. Rapp and P. Englander-Golden, J. Chem. Phys. 40, 573,120 (1964).

(8) K.F. Herzfeld and T.A. Litovitz, Absorption and Dispersion of Ultrasonic Waves, Academic Press, New York, (1959).

(9) R.L. Taylor and S. Bitterman, Rev. Mod. Phys. 41, 26 (1969).

(10) Y. Sato, S.Tsuchiya and K. Kuratani, J. Chem. Phys., 50, 1911 (1969).

(11) R.D. Sharma and C.A. Brau, Phys. Rev. Letters, 19, 1273 (1967).

(12) T. Keneshea, AF Cambridge Research Lab Rept. 67-0221, Environmental Research Paper No. 263, April (1967).

(13) T.I. McLaren and J.P. Appleton, MIT Fluid Mechanics Laboratory Publ. No. 70-10, November (1970).